Studies in Gas-Solid Reactions: Part I. A Structural Model for the Reaction of Porous Oxides with a Reducing Gas

J. SZEKELY AND J. W. EVANS

A structural model is presented for describing the reaction of a porous metal oxide pellet with a reducing gas. It is suggested that the pellet is made up of a large number of grains and the overall rate of reaction is computed by summing the contributions of all these individual grains. The model thus incorporates structural parameters, such as grain size, porosity (pore size distribution) and allows a quantitative assessment of the role played by these quantities in determining the rate of progress of the reaction.

THE reaction of porous metal oxide aggregates with a reducing gas is of considerable technological importance and has consequently received a great deal of attention. A large proportion of these studies was concerned with iron oxide reduction but many other systems have also been extensively studied.

Most of the investigators to data have interpreted their results by using a suitable variant of the "shrinking core model".[1-8] This model, sketched schematically in Fig. 1 is based on the assumption that after some reaction had occurred the solid phase consists of an unreacted core, surrounded by a reacted shell. These two zones are separated by a sharp phase boundary where the chemical reaction takes place. As the reaction proceeds, the reacted shell expands and diffusion of the reactants and products through this region may become one of the rate limiting factors.

The shrinking core model (model based on "topochemical reactions") has been remarkably successful for the interpretation of experimental results; in general, the equations based on this representation described the overall rate in terms of a "driving force" and three sets of resistances, namely:

i) Gas phase mass transfer.

ii) Diffusion of reactants and products through the reacted shell.

iii) Chemical reaction occurring at the interface separating the reacted and the unreacted regions.

Of these quantities, the gas phase mass transfer coefficient and the rate of pore diffusion may be predicted, or at least estimated. The parameters characterizing the chemical kinetics, however, have to be measured experimentally. Indeed, the form of the rate equation and the numerical values of the rate constant served as the principal adjustable parameters which allowed the matching of experimental and "theoretical" results.

While the shrinking core model has been very widely used, it suffers from two major shortcomings:

a) The important postulate of "topochemical reaction", *i.e.*, the existence of a sharp boundary between the reacted and unreacted zones is not universally supported by experimental evidence. In their study of hematite reduction, Gray and Henderson[9] found that the reduced and unreacted sections were separated by a transition zone, which contained both totally reduced and only partially reduced grains. Similar findings were reported by Weisz and Goodwin[10] in their investigation concerned with the combustion of carbon deposits in porous catalysts.

b) Perhaps the most serious drawback of the shrinking core model is the fact that structural effects, such as porosity, grain size, and so forth, are implicitly incorporated in the chemical rate constant and do not appear explicitly. It follows that any measurement made of reduction kinetics is necessarily specific to a given material or even to a given batch of material, and no unique reaction parameters can be assigned to a given ore or sinter. The shrinking core model provides little guidance on the role played by structural parameters in determining the overall reaction rate.

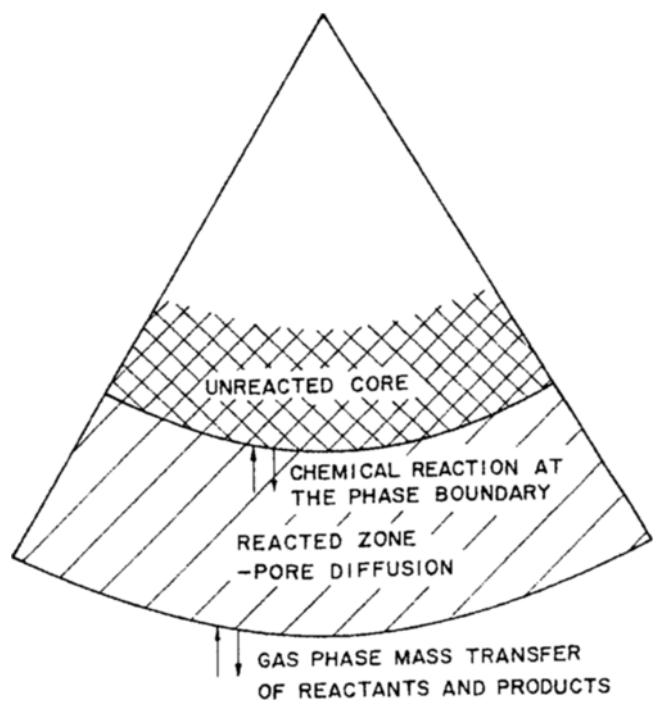

Fig. 1—Schematic representation of the shrinking core model.

J. SZEKELY is Professor of Chemical Engineering and Director, Center for Process Metallurgy at the State University at Buffalo, Buffalo, N. Y. J. W. EVANS, formerly Graduate Student in Chemical Engineering at the State University of New York at Buffalo, is now with the Ethyl Corp., Baton Rouge, La.

Manuscript submitted July 24, 1970.

These apparent shortcomings of the topochemical assumption prompted a number of recent studies,[11-14] of which the work reported by Ishida and Wen[14] is probably the most noteworthy. These authors regarded the porous solid matrix as a homogeneous medium and described the gas-solid reaction in terms of a "homogeneous rate constant." This representation led to a diffuse reaction front but still would not allow the a priori prediction of the reaction rates in terms of structural considerations.

Finally, in a recent paper the authors proposed a structural model[15] for the reaction between a semi-infinite porous medium and a gaseous reactant. Through this model it was possible to identify some of the significant structural parameters, but the geometry chosen precluded direct comparison with measurements.

The work reported in the present series of papers was undertaken with a view of developing a structural model which can be compared directly with experimental measurements. The ultimate objective of the investigation is to define the *physical criteria* that affect the reactivity of porous solids, and hence to define the optimal conditions for effecting these reactions.

In Part I we shall present a mathematical model, which is a further development of that described in the earlier publication, and in the subsequent Part II the predictions based on the model will be compared with experimental measurements obtained, using the system $NiO-H_2$.

FORMULATION

Let us consider a spherical pellet of the solid reactant, made up of a large number of spherical grains of uniform radius, r_s. Let the porosity of the sample be P, and the distance from the center (macroscopic radial coordinate) be designated by R. The sample is brought into contact with a gas, A, with which it reacts to form a solid product and a gaseous product, B.

The following major assumptions are made:

i) The initial physical structure is maintained throughout the reaction, and

ii) the reaction of each grain proceeds from the outside toward the center, so that the position of the reaction front *within each grain* exhibits spherical symmetry—this behavior may be described as the microscopic shrinking core. Thus the rate at which each grain reacts is proportional to the surface area of the reaction front at any given time. The radius of this microscopic reaction front is designated by r, which is a function of time and of R (*i.e.*, radial position within the sample).

The model described above is sketched in Fig. 2 where it is seen that the reactant gas is transferred from the bulk gas stream, diffuses between the grains and then through a solid product layer within each grain and reacts at the spherical reaction interface. The product gas thus generated diffuses back through the solid product layer and between the grains before undergoing a mass transfer step into the bulk gas stream.

At this stage it may be worthwhile to comment briefly on the appropriateness of these assumptions. Assumption i) is restrictive, nonetheless it is thought to be valid for a range of practical conditions. It is agreed that sintering or agglomeration of the reduced phase will occur in many instances, but it is suggested that these more complex situations are best described in terms of an appropriately modified model.

Assumption ii) is thought to represent a reasonable approximation to reality, at least in a macorscopic sense.

Let us now proceed by stating the appropriate conservation equations for the gaseous reactants and products.

A mass balance on component A yields the following differential equation describing diffusion of A between the grains:

$$\frac{D'_A}{R^2}\frac{\partial}{\partial R}\left(R^2\frac{\partial C_A}{\partial R}\right) - (1-P)\rho_m \cdot \mathcal{S} = 0 \qquad [1]$$

where

ρ_m = true molar density of reactant solid.

$\mathcal{S}$ = rate of disappearance of gaseous reactant per mole of initial solid reactant.

D'_A = the effective diffusivity of the gaseous reactant between the grains of the porous solid.

C_A = molar concentration of the gaseous reactant in the interstices between the grains.

A similar equation may be written for the gaseous product:

$$\frac{D'_B}{R^2}\frac{\partial}{\partial R}\left(R^2\frac{\partial C_B}{\partial R}\right) + (1-P)\rho_m \cdot n_s \cdot \mathcal{S} = 0 \qquad [2]$$

where n_s is the moles of B formed by the reaction of one mole of A. Subsequently, n_s will be taken as unity,

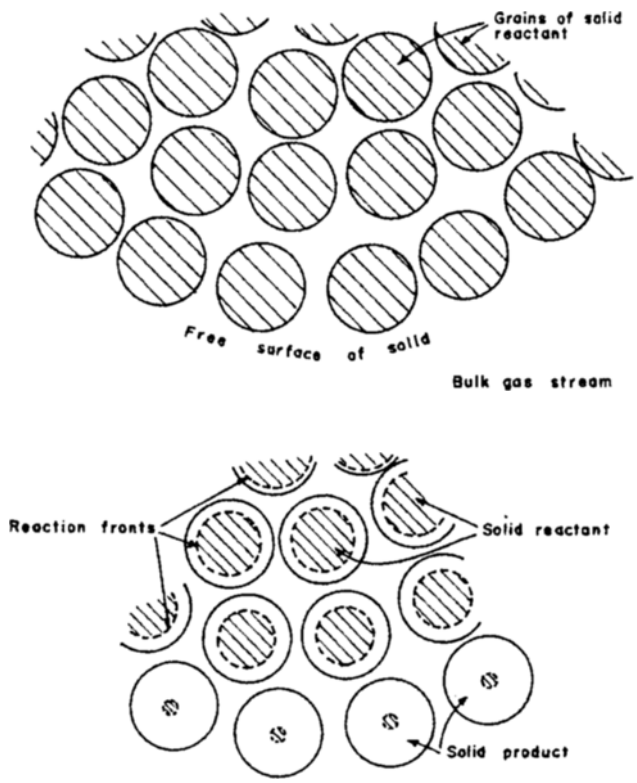

Fig. 2—Schematic representation of the structural model.

but the modification to account for other values of n_s is straightforward.

Eqs. [1] and [2] are valid for equimolar counter diffusion (the present case) or where diffusion between the grains is purely of the Knudsen type. It is to be noted that no accumulation terms appear in the two equations, thus the 'quasi-steady state' assumption is implicit in this formulation. The quasi-steady state assumption is readily justified on physical grounds because the amount of gaseous reactant within the pores is negligible, compared with the net input and the rate of reaction.

Before we can proceed further, the reaction term, $\mathcal{G}$ has to be related to the concentration of the reactants and products and also the rate of progress of the reaction front, within the grains at a particular location, R.

We shall make the following further assumptions:

iii) The reaction between the gas and the solid is of first order in both the forward and reverse directions, and

iv) there is negligible resistance due to diffusion through the product layer *within the grains*; thus the concentration at the reaction surface within a grain is identical with that in the interstices at the same radial coordinate.

The assumption regarding first order kinetics is restrictive, nonetheless it will apply to many systems, in particular it will hold as a reasonable approximation in the vicinity of equilibrium, *i.e.*, in the mixed control regimes. Nonlinear kinetic expressions could be readily accommodated but in view of the much larger demand on computer time this possible refinement was not incorporated at this stage.

Assumption iv) is thought to be reasonable for small grains as the diffusion path through the (porous) grains is very much smaller than the diffusion path through the bulk of the porous solid.

With these assumptions, iii) and iv), the advancement of the reaction front within a grain is written as:

$$\frac{dr}{dt} = -\frac{k}{\rho_m}\left(C_A - \frac{C_A}{K_E}\right) \qquad [3]$$

where k is the chemical reaction rate constant and K_E is the equilibrium constant.

$\mathcal{G}$, the reaction term, may now be readily related to the advancement of the reaction front within a grain, as follows:

For the case where one mole of A reacts with one mole of solid,* we have:

*Ready allowance could be made for other stoichiometries through the use of an appropriate constant of proportionality.

$$4\pi r^2 \cdot \frac{dr}{dt}\rho_m = 4\pi r^2 k\left(C_A - \frac{C_B}{K_E}\right) \qquad [4]$$

Thus

$$= \frac{3r^2 k}{\rho_m r_s^3}\left(C_A - \frac{C_B}{K_E}\right) \qquad [5]$$

On substituting for $\mathcal{G}$ from Eq. [5] into Eq. [1] and [2] we obtain:

$$\frac{D_A'}{R^2}\frac{\partial}{\partial R}\left(R^2\frac{\partial C_A}{\partial R}\right) - 3(1-P)\frac{r^2}{r_s^3}k\left(C_A - \frac{C_B}{K_E}\right) = 0 \qquad [6]$$

$$\frac{D_B'}{R^2}\frac{\partial}{\partial R}\left(R^2\frac{\partial C_B}{\partial R}\right) + 3(1-P)\frac{r^2}{r_s^3}k\left(C_A - \frac{C_B}{K_E}\right) = 0 \qquad [7]$$

Here mention may be made of a more general case where the grains are not of uniform size. Let $f(r_s)\cdot dr_s$ be the weight fraction of grains with radii between r_s and $(r_s + dr_s)$ and assume that f is independent of R. Now

$$\mathcal{G} = \int_0^\infty f \cdot \frac{3\cdot r(r_s)^2}{\rho_m r_s^3}\cdot k\left(C_A - \frac{C_B}{K_E}\right)dr_s \qquad [8]$$

and Eq. [3] becomes:

$$\frac{dr(r_s, R)}{dt} = -\frac{k}{\rho_m}\left(C_A - \frac{C_B}{K_E}\right) \qquad [9]$$

Clearly, this additional sophistication would be appropriate only if accurate information were available on the grain size distribution.

INITIAL AND BOUNDARY CONDITIONS

The initial and boundary conditions for the governing Eqs. [3], [6], and [7] have to express the following physical constraints:

a) the initial position of the reaction front within each grain, *i.e.*, that no reaction had taken place before $t = 0$

b) the fact that the concentration profiles are symmetrical about the center of the pellet, and

c) the continuity of the molar fluxes at the outer surface of the pellet, *i.e.*, diffusive flux across the outer surface of the pellet = convective flux through the "gas film" surrounding the pellet.

These boundary conditions are given in Eqs. [10] through [14]:

$$r = r_s \text{ for all } R \text{ at } t = 0 \qquad [10]$$

$$\frac{\partial C_A}{\partial R} = 0 \text{ at } R = 0 \qquad [11]$$

$$\frac{\partial C_B}{\partial R} = 0 \text{ at } R = 0 \qquad [12]$$

$$D_A'\frac{\partial C_A}{\partial R} = h(C_{A_0} - C_A) \text{ at } R = R_0 \qquad [13]$$

$$D_B'\frac{\partial C_B}{\partial R} = h(C_{B_0} - C_B) \text{ at } R = R_0 \qquad [14]$$

where R_0 is the radius of the spherical sample, h is the mass transfer coefficient from the bulk gas stream to the solid sample, C_{A_0} and C_{B_0} are the concentrations of the gaseous reactant and product in the bulk gas stream.

CORRECTION FOR NONISOTHERMAL BEHAVIOR

In general, the temperature of the pellet will differ from that of the gas stream, because of the heat generated or absorbed by the chemical reaction. For relatively small heats of reaction ready allowance may be made for non-isothermality, by assuming that the pellet is at uniform temperature at any given time;[16] then the unsteady state heat balance yields the following:

$$\frac{dT}{dt} = -\frac{H}{C_p}\frac{d\epsilon}{dt} - \frac{3}{R_0(1-P)\rho_m C_p} \times [h_t(T - T_E) + e\sigma(T^4 - T_E^4)] \quad [15]$$

with

$$T = T_E \text{ at } t = 0 \quad [16]$$

where T and T_E are the pellet and environment temperatures in absolute units, H is the heat of reaction, and the other quantities are defined in the list of symbols.

From the knowledge of $d\epsilon/dt$ the pellet temperature may thus be computed and the property values may then be evaluated at this correct temperature. For the practical system to be considered in Part II, this correction amounted only to a maximum of about 20° to 30°C so that the principal effect was confined to the reaction rate constant.

Eqs. [3], [6], [7], and [15], together with the boundary conditions contained in Eqs. [10] through [14] represent a complete statement of the problem. The subsequent manipulation of these equations and the numerical technique used for their solution is discussed in the subsequent section.

THE TECHNIQUE OF SOLUTION

Rearrangement of the Equations

The governing equations may be rearranged on noting that in the absence of coupled fluxes Eqs. [6] and [7] are not independent and one of them may be eliminated by the following procedure:

Stoichiometry dictates that:

$$D_A' \frac{\partial C_A}{\partial R} = -D_B' \frac{\partial C_B}{\partial R} \quad [17]$$

furthermore on combining Eqs. [6] and [7] we have:

$$D_A' \frac{\partial}{\partial R}\left(R^2 \frac{\partial C_A}{\partial R}\right) = -D_B' \frac{\partial}{\partial R}\left(R^2 \frac{\partial C_B}{\partial R}\right) \quad [18]$$

On integrating Eq. [18] once, with respect to R, and using Eq. [17] yields after a further integration:

$$D_A'(\text{Constant} - C_A) = D_B' C_B \quad [19]$$

which is valid for all values of R.

C_B may now be expressed with the aid of Eqs. [17] and [19] to obtain:

$$C_B = C_{A_0} + \left(\frac{D_A'}{D_B'} - 1\right) C_{A_{R_0}} - C_A \cdot \frac{D_A'}{D_B'} \quad [20]$$

Thus on substitution Eqs. [3] and [6] to [7] are transformed to Eqs. [20] and [21], respectively.

$$\frac{dr}{dt} = -\frac{k}{\rho_m}\left\{C_A\left(1 + \frac{D_A'}{D_B' K_E}\right) - \frac{1}{K_E} \times \left[C_{A_0} + \left(\frac{D_A'}{D_B'} - 1\right) C_{A_{R_0}}\right]\right\} \quad [21]$$

$$\frac{D_A'}{R^2}\frac{\partial}{\partial R}\left(R^2 \frac{\partial C_A}{\partial R}\right) = 3(1-P)\frac{r^2}{r_s^3} k \left\{C_A\left(1 + \frac{D_A'}{D_B' K_E}\right) - \frac{1}{K_E}\left[C_{A_0} + \left(\frac{D_A'}{D_B'} - 1\right) \times C_{A_{R_0}}\right]\right\} \quad [22]$$

In generating a solution, we seek values of C_A (and also C_B) and r, for all values of R and t. However, in order to compare the computed results with experimental data, it is convenient to define a quantity, termed the *extent of reaction* which bears a direct relationship to experimentally measured weight change of the specimen.

The overall extent of reaction ϵ may be expressed as follows:

$$\epsilon = \frac{3}{R_0^3}\int_0^{R_0} R^2\left(1 - \frac{r^3}{r_s^3}\right) dR \quad [23]$$

the quantity $[1 - (r^3/r_s^3)]$ may be considered a *local extent of reaction* and will be designated α. Thus the right side of Eq. [21] is the weighted average value of α.

ϵ is not a function of R, but is, of course, a function of t.

The Numerical Solution

In order to put the governing equations in a finite difference form, let us establish a two-dimensional grid in R and t, designating the mesh spacing in R by ΔR and the time step by Δt.

The values of R at the various grid points will be designated by substituting appropriate numerical values into the index i of the quantity R_i, which now denotes discrete values of the spatial coordinate. The index i is so chosen that:

$$i = 1 \quad \text{at } R = 0$$
$$i = n \quad \text{at } R = R_0 \quad [24]$$

The index of any mesh value of R differs from its neighbors by unity.

Eq. [21] may now be replaced by n equations of the type

$$\frac{dr_i}{dt} = -\frac{k}{\rho_m}\left\{C_{A_i}\left(1 + \frac{D_A'}{D_B' K_E}\right) - \frac{1}{K_E} \times \left[C_{A_0} + \left(\frac{D_A'}{D_B'} - 1\right) C_{A_n}\right]\right\} \quad [25]$$

where the subscripts i denote values of the appropriate variables at radius R_i.

If the values of C_{A_i} were known as a function of time, the set of equations represented by Eq. [25] could be readily integrated, *e.g.* by the Runge-Kutta method.

In order to obtain C_{A_i}, let us recall Eq. [22], which may be written as follows:

$$\left[\frac{D_A'}{R^2}\frac{\partial}{\partial R}\left(R^2\frac{\partial C_A}{\partial R}\right)\right]_{R=R_i} = 3(1-P)\frac{r_i^2}{r_s^3} k \left\{C_{A_i} \times \left(1 + \frac{D_A'}{D_B' K_E}\right) - \frac{1}{K_E}\left[C_{A_0} + \left(\frac{D_A'}{D_B'} - 1\right) C_{A_n}\right]\right\} \quad [26]$$

The left hand side of Eq. [26] may be expressed in a finite difference form as:

$$\frac{\partial}{\partial R}\left(R^2\frac{\partial C_A}{\partial R}\right) = R^2\frac{\partial^2 C_A}{\partial R^2} + 2R\frac{\partial C_A}{\partial R} \approx \frac{R_i^2}{\Delta R^2} \times \left[C_{A_{i-1}} - 2C_{A_i} + C_{A_{i+1}}\right] + \frac{R_i}{\Delta R}\left[C_{A_{i+1}} - C_{A_{i-1}}\right] \quad [27]$$

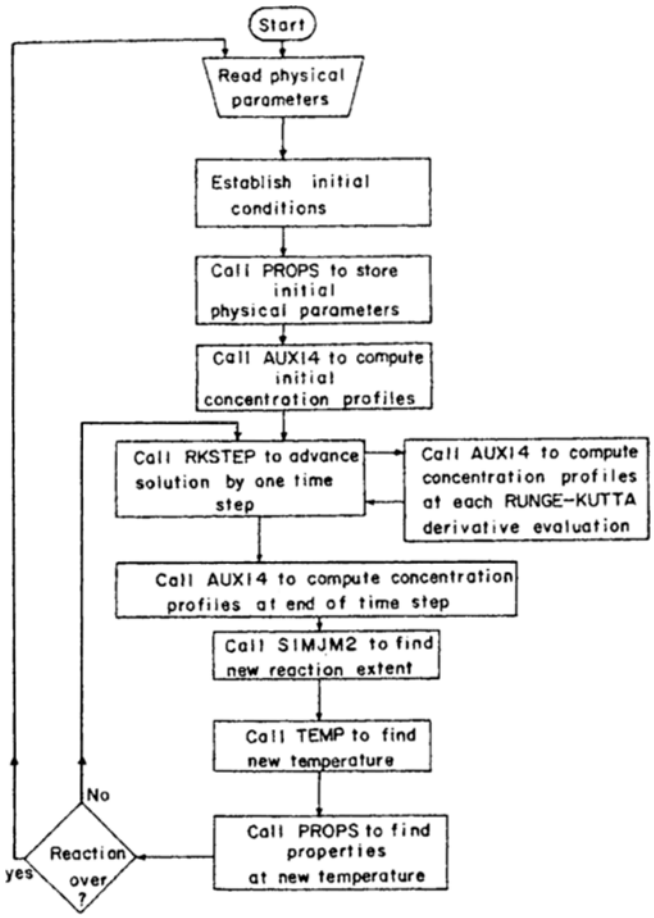

Fig. 3—Block diagram of the computer program.

Here R_i are selected such that the mesh spacing (ΔR) is uniform. On rearrangement Eq. [27] may be written as:

$$\left(\frac{R_i^2}{\Delta R^2} - \frac{R_i}{\Delta R}\right) C_{A_{i-1}} - \left[\frac{2R_i^2}{\Delta R^2} + \mu_i\left(1 + \frac{D'_A}{D'_B K_E}\right)\right] C_{A_i} + \left(\frac{R_i^2}{\Delta R^2} + \frac{R_i}{\Delta R}\right) C_{A_{i+1}} + \frac{\mu_i}{K_E}\left(\frac{D'_A}{D'_B} - 1\right) C_{A_n} = -\frac{\mu_i}{K_E} C_{A_0} \quad [28]$$

where

$$\mu_i = \frac{3(1-P) r_i^2 R_i^2 k}{D'_A r_s^3} \quad [29]$$

Eq. [28] holds for all the internal grid points, *i.e.*, $i = 2, 3, 4, \ldots (n-1)$.

The boundary conditions are also readily expressed in a finite difference form, thus we have:

$$3C_{A_1} - 4C_{A_2} + C_{A_3} = 0 \quad [30]$$

and

$$C_{A_{n-2}} - 4C_{A_{n-1}} + (3 + 2\beta) C_{A_n} = 2\beta C_{A_0} \quad [31]$$

(replacing Eq. [13])

where

$$\beta = \frac{h}{D'_A} \cdot \Delta R \quad [32]$$

Solution may now proceed as follows:

1) Starting with given initial values of r_i and computing the initial values of C_{A_i}, the position of the reaction front is advanced by one time step through the integration of Eq. [25].

2) The resultant new values of r_i may then be substituted into Eqs. [29], [30], and [31] which then yield n simultaneous equations for C_{A_i}, $i = 1, 2, 3, \ldots n$.

3) The new values of C_{A_i} are then used for advancing the reaction front by a further time step.

The actual computation was performed on the Control Data Corporation 6400 computer at the State University of New York at Buffalo, using Fortran IV. The numerical solution of Eq. [26] was performed by a subroutine labeled AUX14. Calling parameters for AUX14 were the n values of R_i and of r_i together with the value of ΔR and for the physical properties h, P, k, D'_A, D'_B, K_E, C_{A_0} and r_s. The n values of C_{A_i} constituted the output from the subroutine.

Another subroutine, RKSTEP, advanced the solution of Eq. [23] by one time step using the fourth order Runge-Kutta technique. This subroutine had as input parameters the present n values of r_i and C_{A_i}, together with k, ρ_m, D'_A, D'_B, K_E, C_{A_0}, and the size of the time step. The new values for r_i constituted the output. For further computational details the reader is referred to the thesis upon which this paper is based.[17]

A block diagram of the computer program is shown in Fig. 3.

COMPUTED RESULTS

In view of the numerical procedure used for solving the governing equations, numerical values were required for the parameters appearing in the equations. These quantities may be divided into two groups, namely:

a) Parameters which are readily available for a given application, or at least, may be easily calculated.

b) Parameters, the evaluation of which required further measurement.

a) Pellet size, R_0, porosity, P, molar density of the solid gaseous reactant and product concentrations, C_{A_0}, C_{B_0}, and the gas film heat and mass transfer coefficients, h_t and h, fall in this first category and therefore no further comment will be made on the techniques used for their evaluation.

b) The parameters that are not very readily measured or evaluated are the reaction rate constant, k, the effective diffusion coefficients, D'_A, D'_B, and the grain size, r_s, or the grain size distribution.

Of these quantities, k, the *reaction rate constant* has to be measured experimentally; k will depend on temperature and on the condition of the surface, but will no longer be affected by the macrostructure of the solid.

D'_A *and* D'_B, *the effective diffusion coefficients*, depend on the tortuosity and are made up of the Knudsen diffusion coefficient and the molecular diffusivity.

On denoting these by D'_{AK} and D'_{BK} respectively, D'_A may be estimated by the Bosanquet interpolation formula:

$$\frac{1}{D'_A} = \frac{1}{D'_{AB}} + \frac{1}{D'_{AK}} \quad [33]$$

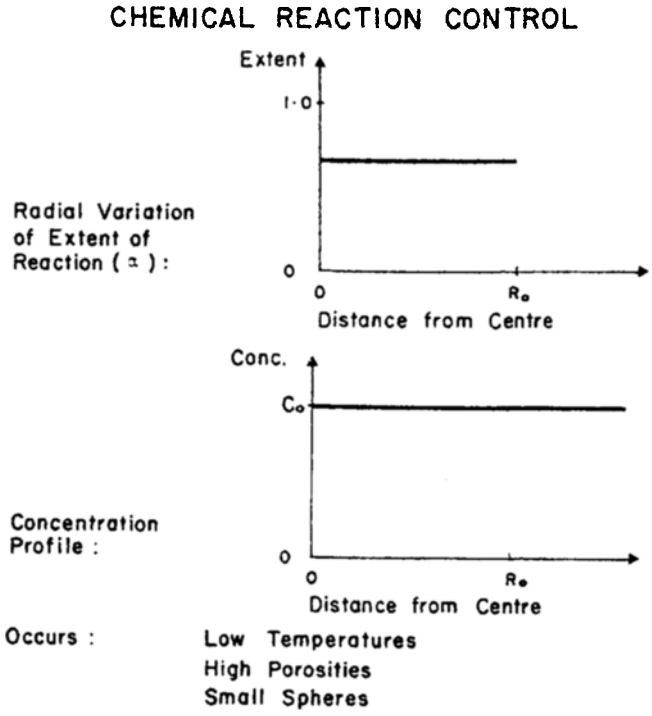

Fig. 4—Typical plot of the local extent of reaction and of the concentration profile for chemical control.

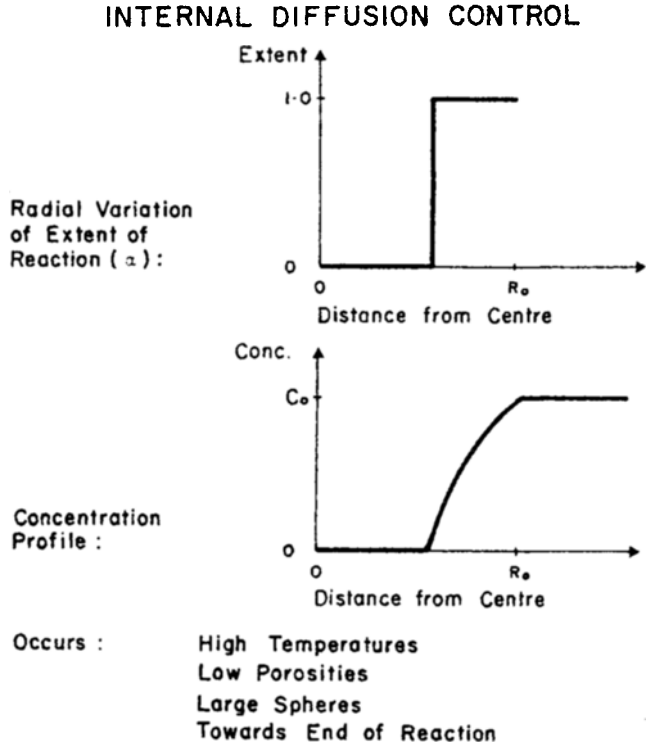

Fig. 5—Typical plot of the local extent of reaction and of the concentration profile for pore diffusion control.

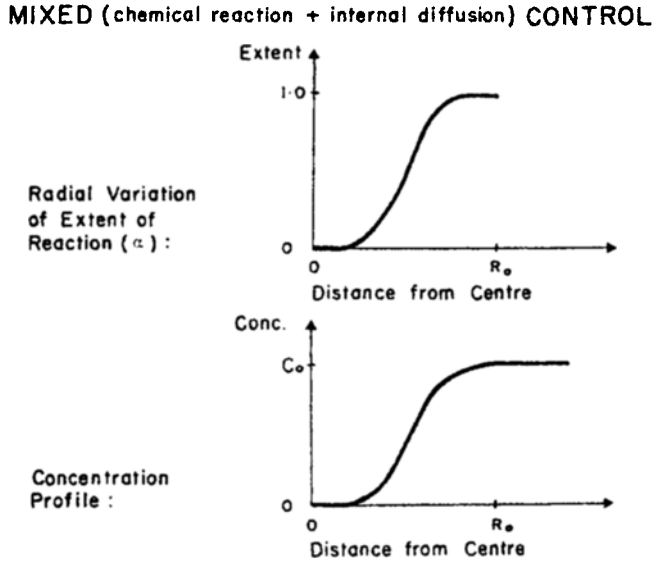

Fig. 6—Typical plot of the local extent of reaction and of the concentration profile for mixed control.

The molecular diffusion coefficient may be estimated from the molecular theory of gases, and the Knudsen diffusion coefficient may also be estimated if the pore size distribution (grain size distribution) and the porosity are known.

Alternatively, D'_A may be measured experimentally through both the reacted and unreacted matrices.

Finally, r_s, the grain size may be either measured directly by electron microscopy, or X-ray diffraction techniques; alternatively, a value for r_s may be deduced from pore size distribution measurements.

It is stressed that the effective diffusion coefficient and the grain size may be strongly interrelated if the component due to Knudsen diffusion is significant.

A further, more detailed discussion will be presented in Part II of the paper regarding the techniques available for estimating and measuring D'_A, k and r_s.

In view of the very large number of parameters that have to enter the computation, any set of computed results will be specific to a particular, given application. At this stage it is thought desirable, to defer the presentation of detailed computed curves to Part II of the paper and to confine ourselves to a discussion of the general features of the solution.

Figs. 4 to 6 show sketches of the concentration profiles and of the spatial distribution of α, the extent of reaction, at some intermediate times, corresponding to various types of asymptotic behavior.

The profiles of α and of C_A, sketched in Fig. 4, correspond to systems where the overall rate is controlled by chemical kinetics; in practical situations chemical kinetics tend to control at low temperatures, at high porosities, and in the case of small pellets. Inspection of Fig. 4 shows that both the concentration and α profiles are uniform.

Fig. 5 shows systems where internal diffusion is the rate controlling step, which is realized at high temperatures, low porosities, and for large pellets. It is seen that the profile of α undergoes a step change from unity to zero at some intermediate value of R, which of course, corresponds to a sharp reaction boundary. Inspection of the concentration profile shows that gradients in concentration are confined to a region between R_0 and the reaction front, *i.e.*, to the reacted shell.

Finally, the behavior of a regime of mixed control (chemical reaction + internal diffusion) is sketched in Fig. 6. It is seen that the profile of α is a smooth curve, a significant portion of which falls between 0 and 1; it follows that this situation corresponds to a

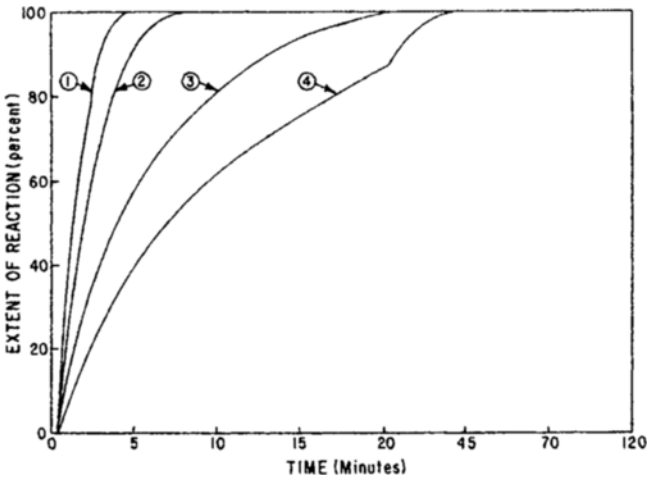

Fig. 7—Plot of the overall extent of reaction against time for nickel oxide reduction with hydrogen. The numbers on the curves correspond to:

No.	Temp, °C	R_0, cm	P, Initial
1	299	0.770	0.729
2	301	1.178	0.734
3	303	0.800	0.384
4	293	1.128	0.384

diffuse reaction zone. The concentration profile shown also reflects this behavior.

Inspection of Figs. 4 to 6 shows that a sharp reaction front exists only in one particular case, when the process is controlled entirely by internal diffusion; in all other cases the reaction zone will consist of a diffuse region, the width of which is determined by the relative magnitude of the various parameters.

Since Figs. 4 to 6, like all preceding illustrations, were sketches of computed behavior, it may be of interest to show actual computed results. This is done in Fig. 7 on a plot of the overall extent of reaction against time. The particular system considered is in the intermediate regime where both diffusion and chemical kinetics are significant. The four curves shown indicate that both porosity and pellet size have a significant effect on the overall reaction rate.

DISCUSSION

In the paper an alternative is proposed to the conventional "shrinking core" model, extensively used for describing the reduction kinetics of solid, porous metal oxides.

The model presented in the paper describes the overall rate of the reaction by summing the contributions from the individual grains that make up the porous solid matrix.

On assuming that the solid structure is not modified in the course of the reaction, the system is represented by two sets of simultaneous differential equations, one set describing the reaction of individual layers of solid grains, and the other describing the diffusion of reactants and products within the porous matrix.

A satisfactory numerical scheme was developed for the solution of these equations, and thus curves were generated giving the appropriate transient concentration profiles and the extent of reaction with time.

The potential attractiveness of the present model is twofold:

a) The profiles generated for the local extent of reaction are in qualitative agreement with experimental findings; a certain combination of circumstances can lead to diffuse reaction zones, whereas there are conditions (when pore diffusion controls) where the reacted and unreacted zones are separated by a sharp reaction boundary.

b) A more significant feature of the model is that it incorporates structural parameters, such as pore diffusion coefficient, grain size, porosity, and the like, into the overall reaction scheme. These quantities may be measured independently, and if adequate information is available on the chemical kinetics, it should be possible to predict the behavior of certain systems from purely physical measurements.

A better understanding of the role played by structural parameters in the overall reaction scheme could lead us to special techniques, or to the modification of existing techniques of solids preparation with a view of achieving optimal performance of the reactor unit in which they are processed. Ultimately, tailor-made structures may be evolved to suit a given, particular gas-solid reaction.

It is noted, that in its present state the model is restrictive, because of the assumption made for the retainment of the original structure.

Within the framework of the model, allowances could be made for structural changes occurring in the course of the reaction. The incorporation of these factors, through additional equations, is quite straightforward in concept but would, of course, increase the complexity of computation. At present there is not enough information available on sintering kinetics for metal-metal oxide systems of interest to make such an effort worthwhile. Nonetheless, future work both in the authors' laboratory and elsewhere, could lead to the construction of more general models.

ACKNOWLEDGMENTS

The authors wish to thank the New York State Science and Technology Foundation for partial support of this investigation. Thanks are also due to the trustees of the C. C. Furnas Fellowship for the support of J. W. E. during the academic year 1969-70.

LIST OF SYMBOLS

C_A, C_B	Gaseous reactant and product molar concentrations within pores
C_{A_0}, C_{B_0}	Gas concentrations in bulk gas stream
$C_{A_{R_0}}$	Reactant gas concentration at pellet surface
C_p	Molar specific heat of pellet
D'_A, D'_B	Effective diffusivities of gaseous reactant and product within porous pellet
e	Total hemispherical emissivity of pellet
f	Grain size distribution function
$\mathcal{G}$	Rate of disappearance of gaseous reactant per mole of initial solid reactant

H	Heat of reaction
h	Mass transfer coefficient
h_t	Heat transfer coefficient
k	Chemical reaction rate constant
K_E	Equilibrium constant
n_S	Stoichiometry coefficient
P	Porosity
R	Radial coordinate within spherical pellet
R_0	Radius of pellet
r	Radius of reaction front within grain
r_S	Radius of grain
T	Pellet temperature
T_E	Environment temperature
t	Time

Greek Letters

α	Local extent of reaction
ϵ	Overall extent of reaction
ρ_m	True molar density of solid reactant
σ	Stefan-Boltzmann constant

REFERENCES

1. S. Yagi and D. Kunii: Proc. 5th Interm. Symp. on Combustion, 1955, p. 231.
2. W. M. McKewan: *Trans. TMS-AIME*, 1962, vol. 224, p. 2.
3. H. W. St. Clair: *Trans. TMS-AIME*, 1965, vol. 233, p. 1145.
4. W. K. Lu and G. Bitsianes: *Trans. TMS-AIME*, 1966, vol. 236, p. 531.
5. R. H. Spitzer, F. S. Manning, and W. O. Philbrook: *Trans. TMS-AIME*, 1966, vol. 236, p. 1715.
6. J. Shen and J. M. Smith: *Ind. Eng. Chem. Fundamentals*, 1965, vol. 4, p. 293.
7. M. Ishida and C. Y. Wen: *Chem. Eng. Sci.*, 1968, vol. 23, p. 125.
8. G. S. G. Beveridge and P. J. Goldie: *Chem. Eng. Sci.*, 1968, vol. 23, p. 913.
9. N. B. Gray and J. Henderson: *Trans. TMS-AIME*, 1966, vol. 236, p. 1213.
10. P. B. Weisz and R. D. Goodwin: *J. Catalysis*, 1963, vol. 2, p. 397.
11. J. M. Ausman and C. C. Watson: *Chem. Eng. Sci.*, 1962, vol. 17, p. 323.
12. D. T. Lacey, J. H. Bowen, and K. S. Basden: *Ind. Eng. Chem. Fundamentals*, 1965, vol. 4, p. 275.
13. A. K. Lahiri and V. Seshadri: *J. Iron Steel Inst.*, 1968, vol. 206, p. 1118.
14. M. Ishida and C. Y. Wen: *Am. Inst. Chem. Eng. J.*, 1968, vol. 14, p. 311.
15. J. Szekely and J. W. Evans: *Chem. Eng. Sci.*, 1970, vol. 25, pp. 1095-1107.
16. D. Luss and N. R. Amundson: *Am. Inst. Chem. Eng. J.*, 1969, vol. 15, p. 194.
17. J. W. Evans: Ph.D. Dissertation, State University of New York at Buffalo, 1970.